UV-irradiation and thermal-annealing studies in amorphous hydrogenated boron nitride thin films

Ian M. Brown, Shu-Han Lin, and Bernard J. Feldman
Departments of Physics and Chemistry and the Center for Molecular Electronics, University of Missouri–St. Louis, St. Louis, Missouri 63121
(Received 3 February 1997)

Both photoproduction and photobleaching of dangling bonds by uv irradiation and thermal annealing were observed by electron spin resonance (ESR) in amorphous hydrogenated boron nitride. A model involving long-range hydrogen diffusion and hydrogen evolution is proposed to account for the ESR spectral line shapes observed after uv irradiation and thermal annealing. A Gaussian distribution of activation energies for the long-range hydrogen diffusion was used to explain the observed decrease in spin susceptibility after thermal annealing. A best fit to the spin susceptibility data gave an average activation energy of 0.0475 eV and a half-width of this Gaussian distribution of 0.027 eV. [S0163-1829(97)06028-1]

Light-induced deep gap states, such as dangling bonds, can play an important role in the electronic properties of amorphous semiconductors. For example, Staebler and Wronski first reported photoproduction of dangling bonds in amorphous hydrogenated silicon that lower the photoconductivity of the material; the photoproduction of dangling bonds was reversible by thermal annealing.[1] Photobleaching has been observed in amorphous hydrogenated silicon nitride[2] and in amorphous hydrogenated carbon;[3] in both studies, the photobleaching was reversible by thermal annealing. We report here both photoproduction and photobleaching of dangling bonds in amorphous hydrogenated boron nitride detected by electron spin resonance (ESR); both effects were not reversible by thermal annealing. And we propose a simple model involving hydrogen diffusion to explain these results.

In a previous paper, we reported ESR results that confirmed the existence of a nanocrystalline as well as an amorphous phase in hydrogenated boron nitride thin films grown by plasma-assisted chemical vapor deposition.[4] The ESR spectra in these as-grown samples consist of a ten-line spectrum and a four-line spectrum superimposed on a broad central line. The ten-line spectrum was assigned to a three-boron (B^{11}) defect site,[5] while the four-line spectrum was associated with a one-boron defect site.[6] Both defect sites are located in the nanocrystalline cubic boron nitride regions, whereas the broad central line is due to dangling bonds in the amorphous hydrogenated boron nitride regions.[4]

A capacitively coupled rf plasma reactor with a rf power of 23 W, a self-bias of 430 V, and a feedstock of 2.0 mTorr diborane, 40 mTorr ammonia, and 358 mTorr hydrogen was used to grow the amorphous hydrogenated boron nitride thin films.[4] Aluminum foil substrates were mounted on the anode for film growth and dilute hydrochloric acid was used to dissolve the aluminum, leaving free-standing thin films that were inserted into an *X*-band ESR spectrometer (Varian E-12). The signal averaging and double integration of the ESR signals were carried out with available software (Scientific Software, Bloomington, IL). The samples were irradiated outside the microwave cavity with a 100-W high-pressure mercury lamp (Osram HBO 100). An 11-cm-long quartz cavity cylinder containing distilled water along with a uv high pass filter (Dow Corning No. 9863) was inserted into the light beam to remove some of the infrared energy. A vacuum oven was used for the thermal annealing.

In Fig. 1, the ESR spectra of amorphous hydrogenated boron nitride are displayed before (b) and after (a) the sample had been exposed to uv light for 2 h at room temperature. The difference between spectra (a) and (b) is also shown, clearly displaying both the photobleaching (decreased ESR signal) occurring in the wings and photoproduction (increased ESR signal) occurring in the center of the line.

In Fig. 2, the ESR spectra of a second amorphous hydrogenated boron nitride sample are displayed before (b) and after (a) the sample had been exposed to uv light for 4 h at room temperature. These spectra in Fig. 2 are quite different from those in Fig. 1, due to (1) a higher concentration of three-boron defect sites and a lower concentration of one-

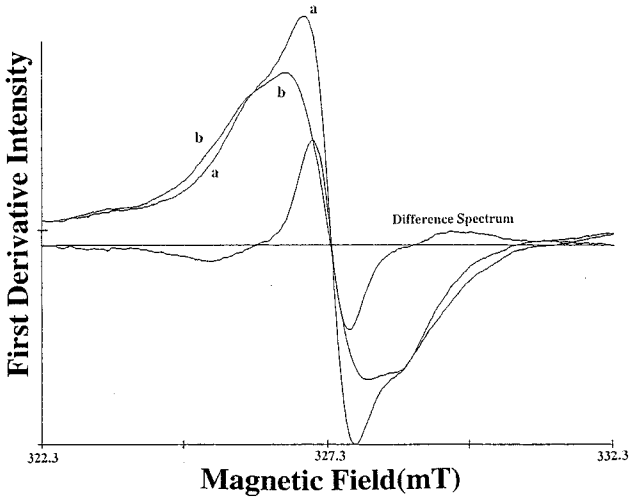

FIG. 1. First derivative ESR line shapes for an amorphous hydrogenated boron nitride thin films observed before uv irradiation (line shape b), after uv irradiation (line shape a), and the difference between line shapes a and b.

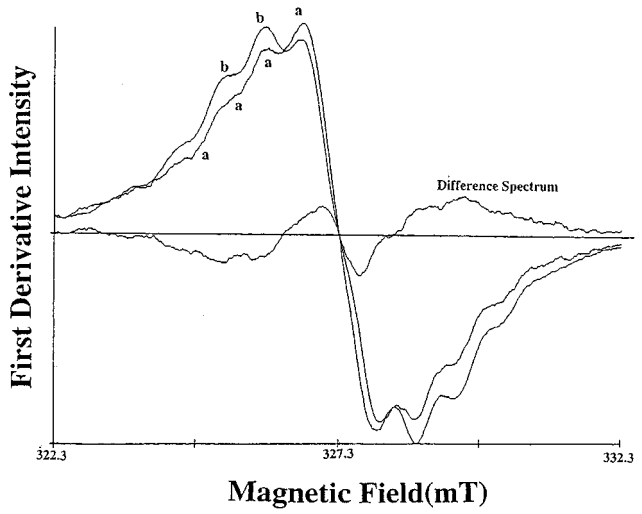

FIG. 2. First derivative ESR line shapes for a second amorphous hydrogenated boron thin film observed before uv irradiation (line shape b), after uv irradiation (line shape a), and the difference between line shapes a and b.

boron sites in the boron nitride nanocrystals and (2) larger hyperfine splittings in the amorphous regions which broaden the central peak. The cause of these variations in defect densities and hyperfine splittings from sample to sample is not known but under investigation.[4] However, the difference spectrum between (a) and (b) shown in Fig. 2 has the same features as the difference spectrum in Fig. 1: photobleaching in the wings and photoproduction in the center of the line.

To investigate the effect of thermal annealing on our samples, we carried out the following experiments. After uv exposure, the second sample was sequentially annealed at temperatures of 300, 400, 500, and 600 °C in a vacuum oven for 1 h. ESR measurements were made after each annealing process; these spectra are displayed in Fig. 3. Figure 4 show the difference spectra between the successive spectra of Fig. 3. It can be seen that after the 300 °C anneal there is photobleaching in the wings and photoproduction in the center

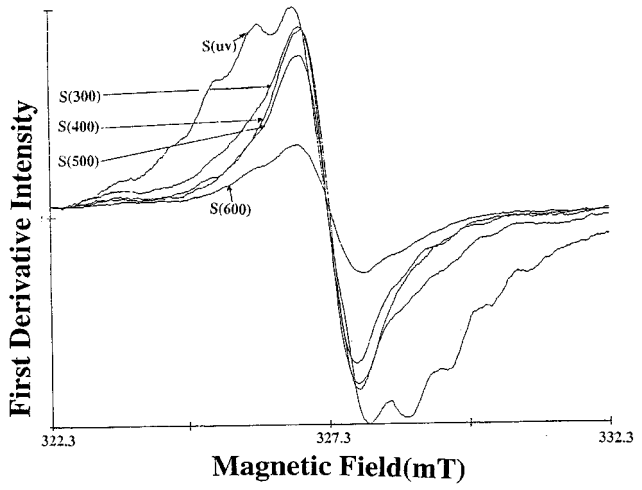

FIG. 3. First derivative ESR line shapes for the second amorphous hydrogenated boron nitride thin film after uv irradiation, $S(\mathrm{uv})$, and after thermal annealing at 300, 400, 500, and 600 °C, namely $S(300)$, $S(400)$, $S(500)$, and $S(600)$, respectively.

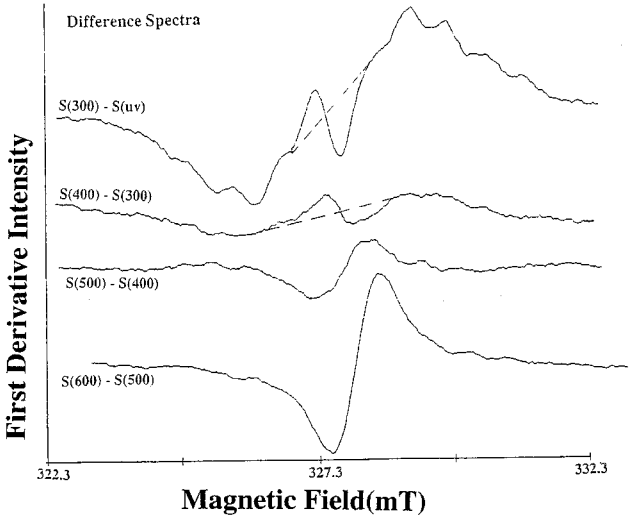

FIG. 4. The following difference first derivative ESR spectra, $S(300)-S(\mathrm{uv})$, $S(400)-S(300)$, $S(500)-S(400)$, and $S(600)-S(500)$. $S(\mathrm{uv})$, $S(300)$, $S(400)$, $S(500)$, and $S(600)$ are the spectra in Fig. 3.

of the line. Similarly, after annealing at 400 °C there are reductions in the wings and an increase at the center of the line. Only after annealing at 500 and 600 °C is there a substantial reduction in the intensity in the wings as well as in the line center.

The data shown in Figs. 3 and 4 indicate both a redistribution and a selective removal of spin susceptibility due to thermal annealing. This behavior suggests a distribution of paramagnetic defect sites, each characterized by an activation energy ϵ. Our model for the decrease in the spin susceptibility due to thermal annealing consists of two assumptions: (1) the spin susceptibility with an activation energy ϵ is removed when $kT \geq \epsilon$, where T is the thermal annealing temperature; and (2) the distribution of spin activation energies is Gaussian:

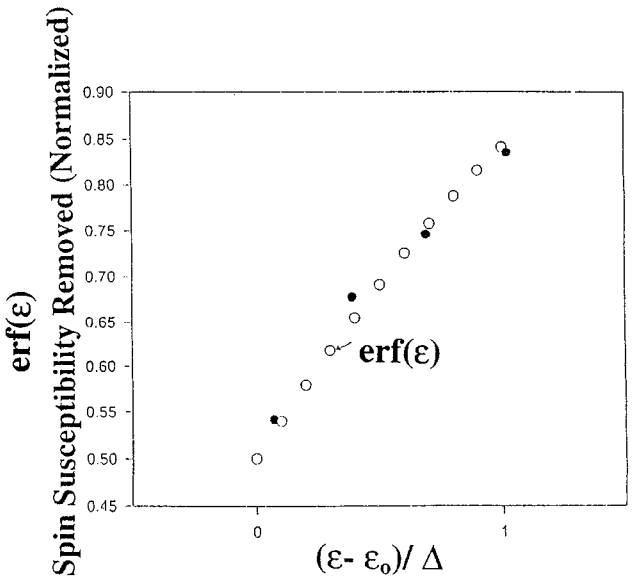

FIG. 5. The measured fraction of spin susceptibility removed on thermal annealing (solid circles) and the calculated best fit from Eq. (3) (open circles) as a function of annealing temperature, $T=\epsilon/k$.

$$n(\epsilon) \propto \exp-[(\epsilon-\epsilon_0)^2/\Delta^2], \quad (1)$$

where $n(\epsilon)$ is the density of spins with an activation energy ϵ, ϵ_0 is the average activation energy, and Δ is the half-width of this Gaussian distribution. Then the spin susceptibility removed after an anneal at temperature T is

$$\chi(T) \propto \int_{\infty}^{kT} \exp-[(\epsilon-\epsilon_0)^2/\Delta^2] d\epsilon, \quad (2)$$

$$\chi(T) \propto \mathrm{erf}(kT). \quad (3)$$

In Fig. 5 the solid circles are the experimental values of the spin susceptibility removed as a function of annealing temperature, $T=\epsilon/k$; the open circles are the best fit of this experimental data to Eq. (3), giving values of $\epsilon_0=0.0475$ eV and $\Delta=0.027$ eV.

Previously, we have reported that on using deuterium instead of hydrogen in the feedstock, the broad ESR spectral line shape narrowed significantly (the peak-to-peak linewidth was reduced from 1.35 to 0.8 mT).[4] This observation proves that the spin intensity in the wings of the ESR line shape is determined by hyperfine interactions with hydrogen. The two main features observed in the ESR spectra due to uv irradiation or thermal annealing, photoproduction in the line center and photobleaching in the wings, can now be explained by long-range diffusion of hydrogen in the sample. The loss of hydrogen from a dangling-bond environment will remove the hydrogen hyperfine coupling constant and consequently shift the spin packet position to the center of the line. The activation energy that characterizes each dangling-bond site will be the activation energy for long-range hydrogen diffusion at that site. Moreover, the net decrease in the spin susceptibility after each anneal means that there is a net reduction in the number of dangling bonds after each anneal, possibly due to a reaction between the dangling bonds and the diffusing hydrogen.

In conclusion, we have observed ultraviolet-radiation photobleaching and photoproduction of dangling bonds in amorphous hydrogenated boron nitride. Thermal annealing produced similar changes in the ESR line shape. A model involving the long-range diffusion of hydrogen is proposed to explain these results. This model accounts for the decrease in intensity in the wings and the increase in intensity in the line center. The model also accounts for the overall decrease in spin susceptibility with increasing annealing temperature by using a Gaussian distribution of activation energies for hydrogen diffusion.

This research was partly supported by the University of Missouri Center for Molecular Electronics.

[1] D. L. Staebler and C. R. Wronski, Appl. Phys. Lett. **31**, 292 (1977).
[2] M. S. Crowder, E. D. Tober, and J. Kanicki, Appl. Phys. Lett. **57**, 1995 (1990).
[3] A. Reyes-Mena, J. Gonzales-Hernandes, and R. Asomoza, Solid State Commun. **86**, 489 (1993).
[4] Shu-Han Lin, I. M. Brown, and B. J. Feldman, Solid State Commun. **96**, 421 (1995).
[5] A. W. Moore and L. S. Singer, J. Phys. Chem. Solids **33**, 343 (1972).
[6] A. Katzir, J. T. Suss, A. Zunger, and A. Halperin, Phys. Rev. B **11**, 2370 (1975).